Effects of precursor chemistry and thermal treatment conditions on obtaining phase pure bismuth ferrite from aqueous gel precursors

A. Hardy [a,b,c,1], S. Gielis [a,1], H. Van den Rul [a,b,1], J. D'Haen [b,d], M.K. Van Bael [a,b,*], J. Mullens [a,1]

[a] *Hasselt University, Laboratory of Inorganic and Physical Chemistry, Institute for Materials Research, Oxide Nanomaterials, Agoralaan, Building D, 3590 Diepenbeek, Belgium*
[b] *IMEC vzw, Division IMOMEC, Diepenbeek, Belgium*
[c] *XIOS Hogeschool Limburg, Department of Applied Engineering Sciences, Diepenbeek, Belgium*
[d] *Institute for Materials Research, Materials Physics, Wetenschapspark 1, 3590 Diepenbeek, Belgium*

Abstract

Phase pure $BiFeO_3$ powders are synthesized by an entirely aqueous solution–gel route, starting from water soluble Fe(III) nitrate or citrate, and Bi(III) citrate as precursors. In order to obtain stable solutions, which transform to homogeneous gels upon drying, the pH is adjusted to 7 and a citric acid content equimolar to the metal ions is selected.

The presence of nitrate strongly accelerates the thermo-oxidative decomposition step of the precursor gel around 200 °C, and the decomposition is finished at a lower temperature for the nitrate containing precursor (460 °C) than without nitrates (500 °C) in dynamic dry air. An oxidative ambient is required to fully decompose the precursor.

The presented synthesis allows very low temperature (400 °C) crystallization of $BiFeO_3$ together with a secondary phase, as shown by high temperature XRD. This parasitic phase remains up to high temperatures, where decomposition of $BiFeO_3$ is observed from 750 °C onwards, and $Bi_2Fe_4O_9$ is formed. However, optimization of the furnace treatment, considering anneal temperatures and heating rates showed that phase pure $BiFeO_3$ can be obtained, with the heating rate being the crucial factor (5 °C/min). The chemical purity of the powders is confirmed by FTIR, and the antiferromagnetic to paramagnetic phase transition is demonstrated by DSC measurements.
© 2009 Elsevier Ltd. All rights reserved.

Keywords: Powders—chemical preparation; Sol–gel processes; Perovskites; X-ray methods; Multiferroic properties

1. Introduction

$BiFeO_3$ is receiving greatly increasing attention recently, due to its multiferroic characteristic, showing both ferroelectric and antiferromagnetic properties with high ferroelectric Curie and Néel temperatures of 830 °C and 370 °C respectively.[1] The lead-free composition and the ferroelectricity make the material suitable for application in random access memory.[2]

The multiferroic property on the other hand enables electric field controlled magnetic data storage, with significant advantages concerning power consumption and downscaling.[3] Phase purity of the $BiFeO_3$ is of importance for high quality of the functional properties. However, $BiFeO_3$ has for a long time been troubled by observations of phase impurities. This is related to the complex phase diagram of Bi_2O_3–Fe_2O_3, with $Bi_2Fe_4O_9$ and $Bi_{25}FeO_{40}$ being the stable compounds surrounding $BiFeO_3$,[4] and to Bi_2O_3 loss during high temperature treatments for long periods.[5] Therefore, the low temperature crystallization which is in general enabled by sol(ution)–gel routes, due to the homogeneous mixing of metal ions on the atomic or molecular scale, shows great promise. Even still, obtaining phase pure $BiFeO_3$ remains challenging, yet recent reports of autocombustion, adjusted Pechini or hydrothermal routes[6–8] demonstrated that the formation of phase pure $BiFeO_3$

* Corresponding author at: Hasselt University, Laboratory of Inorganic and Physical Chemistry, Institute for Materials Research, Oxide nanomaterials, Agoralaan, Building D, 3590 Diepenbeek, Belgium. Tel.: +32 0 11 268307; fax: +32 0 11 268301.

 E-mail addresses: an.hardy@uhasselt.be (A. Hardy), marlies.vanbael@uhasselt.be (M.K. Van Bael).

 [1] Tel.: +32 0 11 268393.

is possible. Different carboxylato complexes, prepared from Fe and Bi nitrate as starting products, were applied as precursors,[7] with or without ethylene glycol as a polymerizer. Ethylene glycol (EG) is toxic, and adds to the organic content of the precursors. Therefore, synthesis routes where EG can be avoided, are most interesting. However without EG, only in the case of malic acid as the complexant, phase pure $BiFeO_3$ was obtained, though the precursor contained an unidentified crystalline species.

Here, we present an aqueous solution–gel route for the preparation of $BiFeO_3$ powders based on citrato complexes, without ethylene glycol. A water based wet chemical synthesis has obvious ecological and economical advantages over solvent based routes. Furthermore, we demonstrate a nitrate-free synthesis route as well, with the advantage of reduced NO_x gas emissions during thermal decomposition. Phase impurities were observed for different heat treatment conditions, but in-depth study of the formation mechanism of $BiFeO_3$ from the precursor, allowed obtaining phase pure $BiFeO_3$. Besides the advantage of high purity and stoichiometry control, provided by chemical synthesis routes, a specific advantage of solution precursors is the possibility to deposit thin films. Here, the avoidance of a crystalline precipitate at the precursor stage is crucial in order to obtain uniform film deposition, without defects such as comets caused by the small scale precipitates on the substrate surface. Therefore, the synthesis route from amorphous precursors for the powders presented here can be valuable for future preparation of thin films from the same precursors.

We present insights into the phase formation of $BiFeO_3$ from a multimetal ion carboxylate gel, through the study of the effects of synthesis and thermal decomposition pathways of the precursor.

2. Experimental details

2.1. Monometal ion precursor synthesis

Starting products for the synthesis are Bi(III)citrate ($BiC_6H_5O_7$, 99.99%, Aldrich), Fe(III)citrate hydrate ($FeC_6H_5O_7 \cdot H_2O$, 98%, 18–20% Fe, Acros), Fe(III)nitrate nonahydrate ($Fe(NO_3)_3 \cdot 9H_2O$, 98.0–101.0%, Alfa Aesar), and citric acid ($C_6H_8O_7$, 99%, Sigma–Aldrich). The exact number of hydrate water molecules in the Fe(III)citrate hydrate starting product is 2.7, as determined by means of TGA.

The Bi(III) precursor is synthesized as reported previously.[9] It has a concentration of ~1.2 mol/l, a molar ratio of citric acid to Bi^{3+} = 1:1, and it contains monoethanolamine ($NH_2(CH_2)_2OH$, 99.5 + %, Aldrich) in a molar ratio of 1.5:1 Bi^{3+}. The pH is adjusted to 7 with concentrated NH_3 (Merck extra pure, 32%) to improve the complexation by deprotonation of the carboxylic acid groups in citric acid.

For Fe(III), a stable citrate precursor with pH 1.5 is prepared with a concentration of 0.7 mol/l by refluxing the required amount of Fe(III)citrate in water at $80\,°C$ overnight. The pH is not increased, as preliminary experiments showed this leads to precipitation. Indeed, from the pM′–pH diagram of Fe(III) in the presence of citrate ligands[10] it can be deduced that $Fe(OH)_3$

forms at higher pH. Also, an Fe(III) nitrate precursor is prepared by simply dissolving $Fe(NO_3)_3$ in water, to obtain a clear and stable solution of 0.4 mol/l. Its pH (~0.5) is not increased, to prevent precipitation due to hydrolysis and condensation of the Fe(III) ion. The low pH of the precursor, however, indicates that hydrolysis reactions are taking place readily.

The monometal ion precursor solutions are filtered using a membrane filter (Gelman sciences, supor, $0.1\,\mu m$) to remove particles, such as dust, impurities and undissolved fractions. Subsequently their exact concentration is determined by ICP–AES (Optima 3000, PerkinElmer).

Precursor solutions are evaporated in an air flushed laboratory furnace at $60\,°C$ for gelation. The gels obtained are crushed and ground manually in an agath mortar before thermal treatment. For the nitrate containing precursor, its strong hygroscopic character turns grinding impossible, and necessitates the use of (ungrounded) small flakes instead of a fine powder for the TGA. In certain cases, the gels are precalcined at $200\,°C$ in the same furnace, and then ground.

2.2. Characterization

Thermo-gravimetric analysis (TGA) is carried out by means of a TA Instruments TGA2950, using typically 4.5 mg of sample powder. As the sample swells up during heating, larger sample masses are not possible. X-ray diffraction (XRD, Bruker D5000, Cu $K\alpha_1$) is used for an off-line study of crystalline phase composition of the samples. Samples for ex situ XRD measurements are prepared by treating 20 mg of the powdered gels, in an alumina combustion boat inside a tube furnace, flushed with a gas of choice (0.4 l/min).

On the other hand, crystallization is also studied in situ, by means of high-temperature XRD (Bruker D8, Cu $K\alpha$, with an Anton Paar heating module). Prior to high temperature XRD analysis, the precursor gels are precalcined at $100–200\,°C$ in a laboratory furnace, to remove part of the organic material, while keeping an amorphous nature. The samples are heated from 300 to $800\,°C$ at $30\,°C/min$, while recording one XRD pattern every $50\,°C$. Recording of each pattern requires an isothermal period of ~7–8 min. A broad peak around $13°2\theta$ is ascribed to the capton windows of the heating module.

Selected powders are characterized by FTIR (Fourier transform infrared spectroscopy, Bruker, Vertex 70, KBr pellets).

Differential scanning calorimetry (DSC) is carried out using 20 mg of bismuth ferrite powder in an aluminum sample pan, while applying a heating rate of $20\,°C/min$ in 50 ml/min N_2 (TA Instruments, Q200 with RSC90 refrigerated cooling system).

3. Results and discussion

3.1. $BiFeO_3$ precursor synthesis

Multimetal ion precursor solutions for $BiFeO_3$ (BFO) are prepared, which are stable and transform to a clear, homogeneous gel upon evaporation, by mixing the Fe(III) and Bi(III) solutions in the desired amounts, followed by adjustment of the pH to 6–7 (Fig. 1. The molar ratio of citric acid to the total
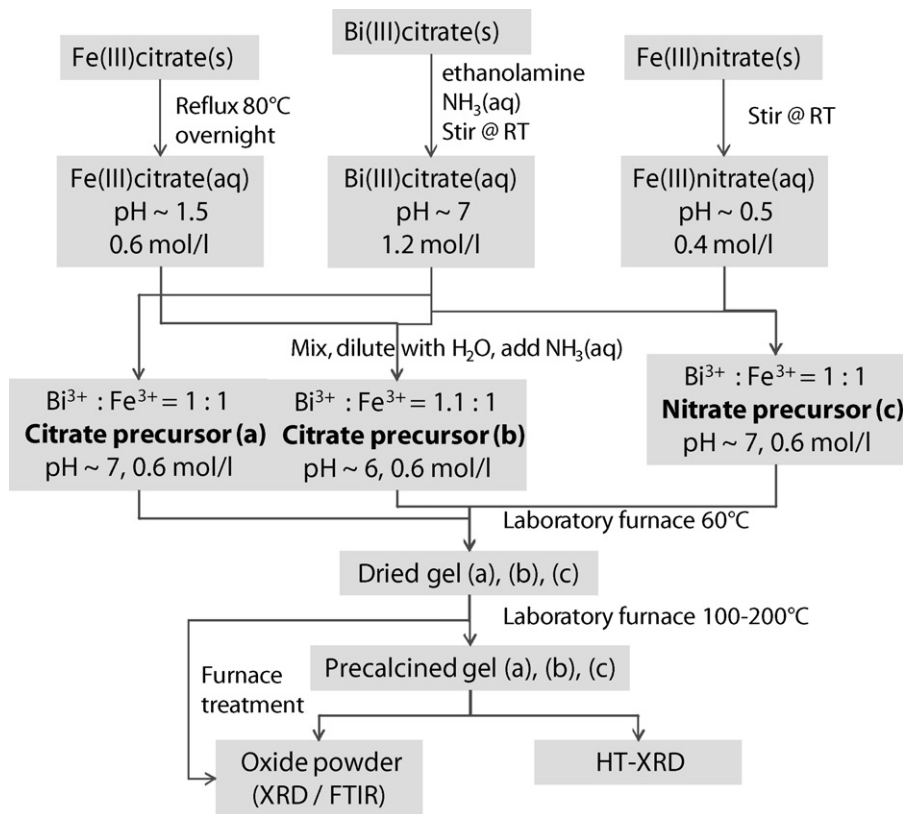
Fig. 1. Synthesis flowchart and application of the precursors in subsequent experiments.

of the metal ions is equal to 1:1 A higher citric acid content also yields stable, gellable solutions in a wide pH range, but leads to redundant organic material that has to be removed by thermal decomposition afterwards. Stoichiometric and 10% Bi excess BFO precursor gels (a) and (b) are prepared from the Fe(III)citrate solution and another stoichiometric BFO precursor gel (c) is prepared using the Fe(III) nitrate precursor solution (Table 1). 10% Bi excess, is added to compensate for eventual bismuth loss during thermal treatment.

3.2. Thermal decomposition of the precursor gels

The thermal decomposition of the precursors is studied by TGA (Fig. 2). A small weight loss is observed around 100 °C, which is ascribed to evaporation of water, absorbed by the precursors during the grinding procedure. Around 200 °C, a strong weight loss is initiated for all precursors, but this decomposition reaction occurs at a much higher rate for the nitrate containing BFO precursor (c) than for the citrate precursors (a, b). In the case of the citrate BFO precursors (a, b), several steps appear to overlap in the temperature region from 200 °C to 500 °C, indi-

cating the occurrence of different thermal processes. The final decomposition steps of the gels show a maximum rate, under the experimental conditions applied here, at 425 °C (nitrate precursor c) or 470 °C (citrate precursor a, b). The weight loss is finished around 460 °C (precursor c) or 500 °C (precursor a, b). The final mass percentage around 35% is relatively high, due to the low citric acid content. The mass percentage remaining after heating up to 800 °C is 37.0% for (a), 33.6% for (b), and 33.6% for (c). The difference between precursor (a) and (b) is explained by the presence of excess Bi in (b), which also results

Table 1
Overview of BiFeO$_3$ multimetal ion precursors.

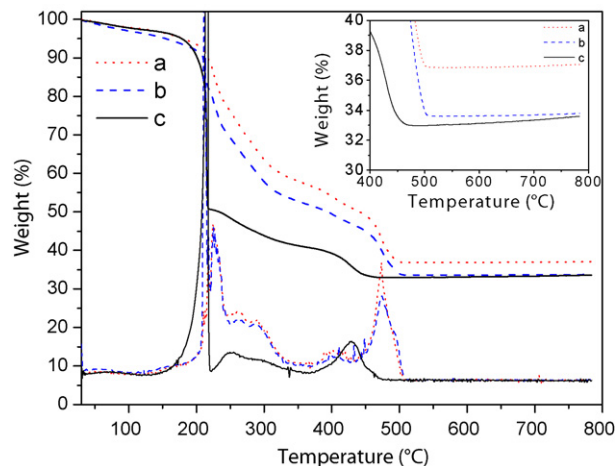|	Bi(III) citrate	Fe(III) citrate	Fe(III) nitrate	10% Bi excess
Precursor a	X	X		
Precursor b	X	X		X
Precursor c	X		X	

Fig. 2. TGA and DTG (20 °C/min, 70 ml/min dry air) of precursors (a), (b) and (c) for BiFeO$_3$.

in a higher content of monoethanolamine, being decomposed during the thermal treatment. Remarkably, precursor (c) shows a stronger increase of the weight percentage between 460 and 780 °C from 23.2% to 33.6% (insert in Fig. 2). This indicates a reaction of the sample with the ambient (dry air), attributed to the oxidation of metallic bismuth, formation of which was observed for bismuth citrate gels before.[11] The reduction of Bi^{3+} in the gel during decomposition, can be related to the violent decomposition reaction occurring around 200 °C, accompanied by ∼45% of weight loss. This temperature range coincides with the temperature range for ammonium nitrate decomposition (210 °C[12]). Self-heating results from the exothermic nature, leading to an apparent acceleration of the decomposition. Secondly, there may also be a contribution of an autocombustion reaction, with the nitrate acting as the oxidizer and the citrate as the fuel. The evaporation of large amounts of decomposition gases, such as CO,[11,13] creates a local oxygen deficient atmosphere, and leads to the reduction of the Bi(III) ion, and eventually the Fe(III) ion as well. After all the organic components are decomposed, the oxidative conditions are restored and the subsequent re-oxidation leads to the weight increase. This indicates severe phase segregation in the case of the nitrate containing precursor, which is a strong disadvantage. However, as the kinetics of this reaction are governed by self-heating, the sample size can have a strong effect. Indeed, TGA analyses of different sample masses of precursor (c) showed that immediately after the violent reaction at 200 °C, a sample mass of 2.3 mg leaves 57%, while a sample mass of 4.6 mg leaves 50%. This may be related to less self-heating and a more efficient heat removal for a smaller sample mass. Note that variations of a few percent are observed in replicate measurements, which are attributed to differences of sample distribution in the sample pan, related to the hygroscopicity, necessitating the use of sample flakes. This variability between replicates was not observed for purely citrate precursor gels (a and b), ground to a fine powder.

The use of different ambients, as shown for citrate precursor (a) in Fig. 3, leads to a similar profile in TGA and DTG until the final decomposition step. The latter, however, is strongly accelerated with increasing oxygen content, as seen in the DTG (Fig. 3). Both oxygen and dry air (20% O_2 + 80% N_2) lead to
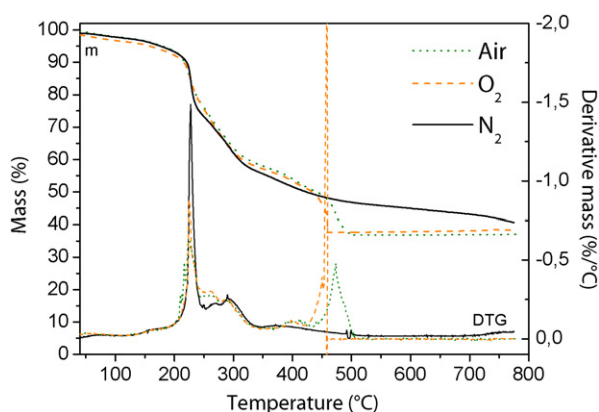
full decomposition of the $BiFeO_3$ precursor, but in N_2 it is not decomposed completely even after heating up to 800 °C. The effect of the ambient on the final decomposition step with onset around 430 °C indicates that combustion is necessary to remove all organic components at reasonable temperatures. Controlling the oxygen partial pressure in the ambient will only affect the last step, and therefore the decomposition cannot be accomplished at lower temperatures by changing the ambient.

Application of a lower heating rate, leads to an apparent shift of the decomposition steps to lower temperature, as demonstrated for 5, 10 and 20 °C/min for the precursor gel (a) (not shown): The maximum rate of the final decomposition step is observed at 400 °C for 5 °C/min, at 450 °C for 10 °C/min and at 470 °C for 20 °C/min heating rate.

From these experiments, it can be inferred that a heat treatment at ∼400 °C to the least, will be required to transform the gel into the oxide, and the presence of oxygen will enhance its kinetics. It is concluded from the study of the precursor's decomposition mechanism that reduction of metal ions, most probably Bi(III), can occur and is followed by re-oxidation after removal of the organic matrix. This is highly undesirable, as it leads to phase segregation.

3.3. In situ study of oxide crystallization

The oxide crystallization was followed in situ using HT–XRD, as described in the experimental section, but only the patterns taken at 400, 600 and 800 °C are shown in Fig. 4, as the main transformations are observed here.

At 400 °C, the crystallization of the powders is first observed (Fig. 4a, b and c). The rhombohedral $BiFeO_3$ phase (JCPDS 86-1518, ICSD #82614) is observed, together with one diffraction peak of a secondary phase at 27.5°2θ (precursor a and b). This secondary phase is attributed to $Bi_{25}FeO_{40}$ in literature,[4] and the reference pattern JCPDS 46-0416. However, other bismuth rich phases such as $Bi_{24}Fe_2O_{39}$ (JCPDS 42-0201), $Bi_{24}(Bi_{1.04}Fe_{0.84})O_{40}$ (JCPDS 82-1316) and $Bi_{12}(Bi_{0.5}Fe_{0.5})O_{19.5}$ (JCPDS 77-0568) can also explain the observed diffraction peak. Excess Bi (precursor b) and the

Fig. 3. TGA and DTG of the stoichiometric citrate precursor gel (a) in different ambients (20 °C/min, 70 ml/min).
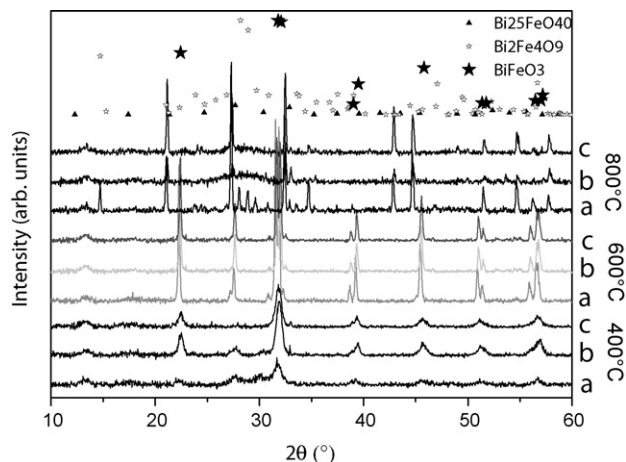

Fig. 4. HT–XRD of $BiFeO_3$ citrate precursor gels (a) and (b) and nitrate–citrate precursor gel (c) at the temperatures indicated.
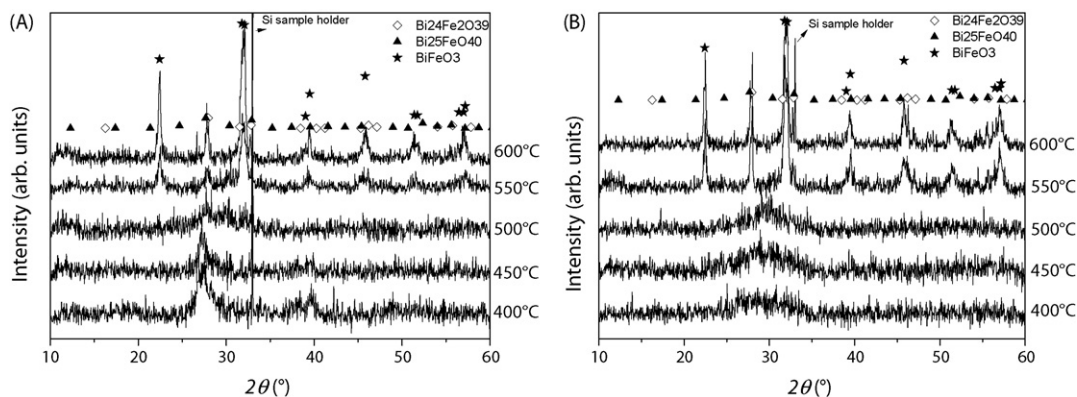
Fig. 5. Ex situ XRD patterns after thermal shock treatment of gel (a) at the indicated temperatures in dry air, A) gel dried at 60 °C, B) gel precalcined at 200 °C.

presence of nitrate (precursor c) enhance the low temperature $BiFeO_3$ crystallization, demonstrated by the more pronounced diffraction peaks compared to precursor a. This is related to the high Bi ion mobility, which contributes to ion diffusion required for crystallization (precursor b), and to the self-heating effect in the nitrate containing precursor (c).

During further heating, the $BiFeO_3$ and secondary phase diffraction peaks increase in intensity and the FWHM decreases, indicating an increase of the amount of crystalline material and of the crystallite size (Fig. 4d, e, f). No remarkable difference exists between the different precursors anymore at 600 °C, since the higher temperature leads to sufficient ion mobility independent of the Bi concentration, and the decomposition of all the precursor gels is completed.

During further heating, starting from 750–800 °C the patterns show strong changes (Fig. 4g, h, i). First of all $BiFeO_3$'s peaks (JCPDS 86-1518) disappear entirely, while new peaks appear that can be attributed to $Bi_2Fe_4O_9$ (JCPDS 74-1098). This is in agreement with literature, reporting the thermodynamic instability of $BiFeO_3$ leading to formation of $Bi_2Fe_4O_9$ and $Bi_{25}FeO_{39}$ already at relatively low temperatures.[4,14,15]

As a conclusion, the aqueous citrato precursor route allows low temperature crystallization of $BiFeO_3$. However, the conditions of static air ambient and stepwise heating during the HT–XRD measurement did not allow formation of phase pure $BiFeO_3$ independent of the precursor's composition and in spite of the strong differences in their thermal decomposition. The observed difficulty of obtaining phase pure $BiFeO_3$ appears to agree with the literature as described in the introduction section.

3.4. Preparation of phase pure $BiFeO_3$

As the presence of nitrate in the precursor provided no advantage for obtaining phase pure $BiFeO_3$ in contrast with its effect on the thermal decomposition of the gel, and as secondary phases observed were Bi rich, only the stoichiometric citrate precursor was selected for further study in order to obtain phase pure $BiFeO_3$ by controlling ambient and heating profile (see Table 2).

A high heating rate was reported to be advantageous for obtaining phase pure $BiFeO_3$ thin films,[4] and therefore thermal shock treatment was carried out. The effect of precalcination was taken into account as well, as in this way the organics,

possibly slowing down the crystallization, are already partially decomposed beforehand (Fig. 5A and B). However, at 600 °C, besides rhombohedral $BiFeO_3$, a secondary phase is observed in XRD at 27.8°2θ (Fig. 5A and B) and it is ascribed to $Bi_{25}FeO_{40}$, similar to the HT–XRD patterns. As 600 °C may be too high a temperature considering the thermodynamic stability of $BiFeO_3$,[14,15] lower temperatures were studied. Without precalcination, from 400–500 °C a broad diffraction peak is observed at 27.3°2θ, 38.2 and 39.6 °2θ (Fig. 5A) with decreasing intensity as a function of anneal temperature. These are ascribed to metallic Bi (JCPDS 44-1246), originating from the reduction of Bi(III) ions by the decomposition gases. Metallic Bi is not formed if precalcination is carried out (Fig. 5B), since after precalcination less organic material is present during the thermal shock treatment, as confirmed by FTIR (not shown). At higher temperatures, the metallic bismuth is oxidized again and might cause the formation of the bismuth rich secondary phase at 550 °C ($Bi_{25}FeO_{40}$ or $Bi_{25}Fe_2O_{39}$ at 27.5 and 39.7°2θ). Even though metallic Bi was not formed for the precalcined gel, $BiFeO_3$ is formed in the presence of the same secondary phase.

The FTIR spectra (Fig. 6) as a function of anneal temperature after precalcination, show the evolution of organic
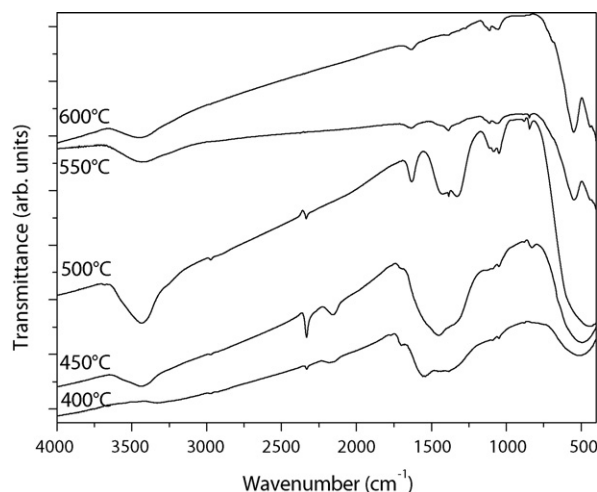

Fig. 6. FTIR spectra of powders obtained by thermal shock treatment of precalcined precursor gel (a) as a function of temperature in dry air.

Table 2
Experimental conditions in the study of $BiFeO_3$ powder preparation.

	Pretreatment	Heating rate	Temperature	Ambient	Result	
					$BiFeO_3$	Secondary phase
1	60 °C	TS	400 °C	DA	−	+
2	60 °C	TS	450 °C	DA	−	+
3	60 °C	TS	500 °C	DA	−	+
4	60 °C	TS	550 °C	DA	+	+
5	60 °C	TS	600 °C	DA	+	+
6	200 °C	TS	400 °C	DA	−	−
7	200 °C	TS	450 °C	DA	−	−
8	200 °C	TS	500 °C	DA	−	−
9	200 °C	TS	550 °C	DA	+	+
10	200 °C	TS	600 °C	DA	+	+
11	**200 °C**	**5 °C/min**	**600 °C**	**DA**	**+**	**−**
12	200 °C	20 °C/min	600 °C	DA	+	+

species in the wavenumber range from 1750–1250 cm^{-1}. The species causing these bands, change as a function of temperature. High temperature stable amides or (oxy)carbonates are formed, which are accompanied by adsorbed CO and CO_2 at 2200 and 2400 cm^{-1}.[13] Finally, the carbon containing species are completely removed at 550 and 600 °C respectively, even though from TGA a lower temperature was derived for full decomposition. This can be due to the isothermal period during annealing being too short, to different experimental conditions such as heating rate, sample amount, air flow and furnace type, or to a higher sensitivity in FTIR. Meanwhile, the oxide crystallization is indicated by the changes of the M–O bands below 1000 cm^{-1} starting from 550 °C, where crystalline perovskite vibrations are observed around 550 cm^{-1}.[16] (Fig. 6).

Precalcination lowers the organic content and leads to less intense decomposition reactions at the anneal temperature. A similar effect can be expected if a lower heating rate is used. As HT–XRD showed no decomposition of $BiFeO_3$ at 600 °C and as FTIR showed it is sufficient to remove organics and (oxy)carbonates, this temperature was selected. Both thermal shock and 20 °C/min heating rate led to the formation of secondary phase(s) together with $BiFeO_3$ (Fig. 7). Applying a heating rate of 5 °C/min on the other hand, reproducibly yields phase pure $BiFeO_3$. Using a slow heating rate reduces overlap between different decomposition reaction steps, allows gradual decomposition of organic ligands and residues formed from them, as well as controlled self-heating. These combined effects provide better control over the local ambient experienced by the metal ions and over their mobility, which is high for Bi^{3+}. As these factors control phase segregation,[11] this explains the crystallization of phase pure $BiFeO_3$.

The antiferromagnetic to paramagnetic second order phase transition was demonstrated for the phase pure powder by DSC measurement (Fig. 8). The enthalpy associated with this transition is very small (0.3 kJ mol^{-1}),[17] which makes it difficult to observe. Comparison with a blank measurement, however, allowed determining the ordering or Néel temperature to be 365 °C, which is in good agreement with recent reports.[7,18,19] This result shows that the synthesized powder has functional properties as well, besides merely being phase pure.
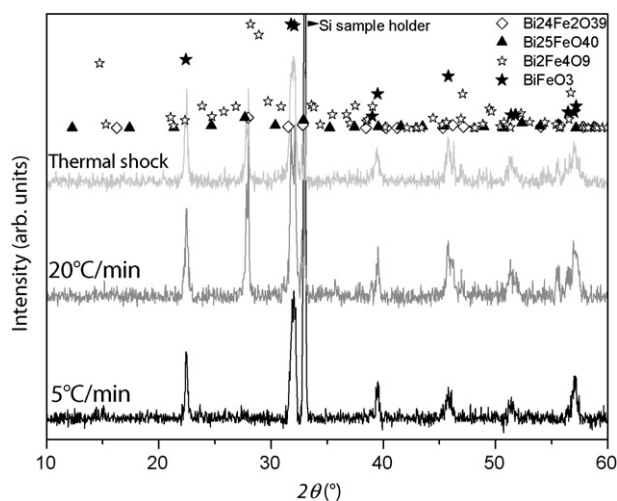

Fig. 7. Ex situ XRD patterns of precursor gel (a) precalcined at 200 °C after heat treatment applying different heating rates up to 600 °C, 30 min isothermal in dry air.
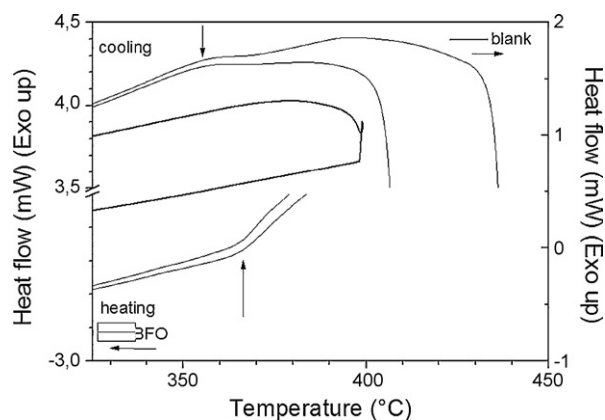

Fig. 8. DSC trace showing the weak signal of the antiferromagnetic to paramagnetic phase transition for BFO by comparison with a blank measurement of an empty sample pan.

4. Conclusion

Entirely aqueous synthesis routes have been shown to allow preparation of gel precursors for $BiFeO_3$, starting from citrate and nitrate salts of Bi^{3+} and Fe^{3+}. From thermo-gravimetric analysis it was concluded that the addition of nitrate in the gels accelerates decomposition and leads to full decomposition at lower temperatures. This is explained by the self-heating effect due to NH_4NO_3 decomposition and by the autocombustion reaction in the nitrate–citrate system. However, both nitrate–citrate and citrate gels showed a bismuth rich phase impurity in high-temperature XRD. Experiments with ex situ heat treatment of the precursor gels under controlled ambients and heating rates, showed that a high heating rate always leads to phase impurity independent of precalcination or anneal temperature. Both factors, however, did affect the removal of organic components from the gel: precalcination at $200\,^\circ C$ and increase of the anneal temperature lead to a stronger progression of the decomposition, as was evidenced by FTIR. Finally, by means of a slow heating rate ($5\,^\circ C/min$) phase pure $BiFeO_3$ was obtained at $600\,^\circ C$. The slow heating rate allows gradual decomposition, and therefore control over the local ambient and the self-heating effect. This in turn affects the metal ion's oxidation state and mobility, finally allowing to avoid the segregation of bismuth rich species. The phase pure powder showed a Néel transition at $365\,^\circ C$.

Acknowledgements

References

1. Wang, J., Neaton, J. B., Zheng, H., Nagarajan, V., Ogale, S. B., Liu, B. *et al.*, Epitaxial $BiFeO_3$ multiferroic thin film heterostructures. *Science*, 2003, **299**, 1719–1722.
2. Scott, J. F., Applications of modern ferroelectrics. *Science*, 2007, **315**, 954–959.
3. Spaldin, N. A. and Ramesh, R., Electric-field control of magnetism in complex oxide thin films. *MRS Bull.*, 2008, **33**, 1047–1050.
4. Tyholdt, F., Jorgensen, S., Fjellvag, H. and Gunnaes, A. E., Synthesis of oriented $BiFeO_3$ thin films by chemical solution deposition: Phase, texture, and microstructural development. *J. Mater. Res.*, 2005, **20**, 2127–2139.
5. Yuan, G. L., Or, S. W., Liu, J. M. and Liu, Z. G., Structural transformation and ferroelectromagnetic behavior in single-phase $Bi_{1-x}Nd_xFeO_3$ multiferroic ceramics. *Appl. Phys. Lett.*, 2006, **89**, 052905.
6. Chen, C., Cheng, J. R., Yu, S. W., Che, L. J. and Meng, Z. Y., Hydrothermal synthesis of perovskite bismuth ferrite crystallites. *J. Cryst. Growth*, 2006, **291**, 135–139.
7. Selbach, S. M., Einarsrud, M. A., Tybell, T. and Grande, T., Synthesis of $BiFeO_3$ by wet chemical methods. *J. Am. Ceram. Soc.*, 2007, **90**, 3430–3434.
8. Ghosh, S., Dasgupta, S., Sen, A. and Maiti, H. S., Low temperature synthesis of bismuth ferrite nanoparticles by a ferrioxalate precursor method. *Mater. Res. Bull.*, 2005, **40**, 2073–2079.
9. Hardy, A., Mondelaers, D., Van Bael, M. K., Mullens, J., Van Poucke, L. C., Vanhoyland, G. *et al.*, Synthesis of $(Bi,La)_4Ti_3O_{12}$ by a new aqueous solution–gel route. *J. Eur. Ceram. Soc.*, 2004, **24**, 905–909.
10. Kragten, J., *Atlas of Metal–Ligand Equilibria in Aqueous Solution*. Chichester, Horwood, 1978.
11. Hardy, A., Vanhoyland, G., Geuzens, E., Van Bael, M. K., Mullens, J., Van Poucke, L. C. *et al.*, Gel structure, gel decomposition and phase formation mechanisms in the aqueous solution–gel route to lanthanum substituted bismuth titanate. *J. Sol–Gel Sci. Technol.*, 2005, **33**, 283–298.
12. Lide, D. R., *CRC Handbook of Chemistry and Physics (83rd edition)*. CRC Press, 2002–2003.
13. Hardy, A., Van Werde, K., Vanhoyland, G., Van Bael, M. K., Mullens, J. and Van Poucke, L. C., Study of the decomposition of an aqueous metal–chelate gel precursor for $(Bi,La)_4Ti_3O_{12}$ by means of TGA–FTIR, TGA–MS and HT–DRIFT. *Thermochim. Acta*, 2003, **397**, 143–153.
14. Selbach, S. M., Einarsrud, M. A. and Grande, T., On the thermodynamic stability of $BiFeO_3$. *Chem. Mater.*, 2009, **21**, 169–173.
15. Carvalho, T. T. and Tavares, P. B., Synthesis and thermodynamic stability of multiferroic $BiFeO_3$. *Mater. Lett.*, 2008, **62**, 3984–3986.
16. Fruth, V., Mitoseriu, L., Berger, D., Ianculescu, A., Matei, C., Preda, S. *et al.*, Preparation and characterization of $BiFeO_3$ ceramic. *Prog. Solid State Chem.*, 2007, **35**, 193–202.
17. Selbach, S. M., Tybell, T., Einarsrud, M. A. and Grande, T., The ferroic phase transitions of $BiFeO_3$. *Adv. Mater.*, 2008, **20**, 3692–3696.
18. Ghosh, S., Dasgupta, S., Sen, A. and Maiti, H. S., Low-temperature synthesis of nanosized bismuth ferrite by soft chemical route. *J. Am. Ceram. Soc.*, 2005, **88**, 1349–1352.
19. Kumar, M. M., Palkar, V. R., Srinivas, K. and Suryanarayana, S. V., Ferroelectricity in a pure $BiFeO_3$ ceramic. *Appl. Phys. Lett.*, 2000, **76**, 2764–2766.